

Comparison of metal-amino acid interaction in Phe-Ag and Tyr-Ag complexes by spectroscopic measurements

Achintya Singha¹, Swagata Dasgupta² and Anushree Roy¹

¹*Department of Physics, Indian Institute of Technology, Kharagpur 721302, India*

²*Department of Chemistry, Indian Institute of Technology, Kharagpur 721302, India*

Abstract

In this article, we have compared the metal-amino acid interactions in Tyr-Ag and Phe-Ag complexes through pH dependent SERS measurements. By analyzing the variation in relative intensities of SERS bands with the pH of the amino acid solution, we have obtained the orientation and conformation of the amino acid molecules on the Ag surface. The results obtained from our experimental studies are supported by the the energy minimized strucutres and the observed charge distributions in different terminals of the molecules. This, in a way, shows that SERS measurements not only exhibit the interaction of the amino acid molecules with Ag clusters but also demonstrate their orientation around it. We have addressed a long standing query on whether the amine group is directly attached with Ag surface along with the carboxylate group and π -electrons in these systems. In addition, pH dependent optical absorption and transmission electron microscopy measurements have been performed to understand the required conditions for the appearance of the SERS spectra in the light of the aggregation of metal particles and the number of hot sites in the sol. Our results confirm that the formation of hot sites in the sol plays a direct role to form a stable Ag-ligand complex. Furthermore, the interaction kinetics of metal-amino acid complexes have been analyzed via both Raman and absorption measurements.

Keywords : metal-amino acid interaction, SERS, optical absorption

I. INTRODUCTION

Spectroscopic studies of amino acids adsorbed on metal surfaces are important because they can provide an insight into the nature of metal-biopolymer interactions [1, 2, 3, 4, 5]. A number of articles have shown that amino acids with small side chains, for example, Glycine (Gly), Alanine(Ala), interact with metal colloids through both the amine and carboxylate terminals [2]. On the other hand, for Phenylalanine (Phe), Tyrosine (Tyr), Tryptophan (Trp), Histidine (His), Leucine (Leu), Glutamic acid (Glu), and Aspartic acid (Asp), the adsorption occurs through the carboxylate group. However, no conclusion is drawn regarding the amine- silver interaction [2, 3].

Surface enhanced Raman scattering (SERS) is an extremely sensitive technique for monitoring the adsorption of species of very low concentration and for characterizing the structure and orientation of the adsorbed species on the rough metal surface [6]. Nonresonance SERS is primarily sensitive to the species attached to the metal surface or present within a few Angstroms of the metal-dielectric interface. Both electromagnetic field and adsorbate-surface chemical interactions are responsible for Raman signal enhancement. The ‘surface selection rules’ and the SERS intensity of a particular Raman band determine the average orientation of functional groups of the adsorbates on the metal surface [2]. In conjunction with optical absorption measurements it has been shown that the single metal cation does not exhibit any SERS effect. Complexation with an organic substance is necessary for signal enhancement [7]. The colloid activation by chemical treatment brings the primary metal particles close together building up ‘hot sites’ that are SERS active in an electromagnetic field of visible wavelength. ‘Hot sites’ are located at interstitial positions between metal particles and the number of such positions scale with the number of particles. In the second step, the activating molecules of very low concentration are bound to the metal surface and form the complex [7]. Despite well-documented limitations, the spectral ‘richness’ in SERS arises not only from the inherent sensitivity of the process, but also from the ability of this technique to determine the interactions in the metal-adsorbate complex and the relative orientation and conformation of the adsorbed molecules on the metal surface.

The structural difference between Phe and Tyr is in the presence of only one -OH group in the para position of the aromatic ring in the latter [Fig 1]. In solution, depending on the pH values [$pK_1 = 2.58$ and $pK_2 = 9.24$] the majority of Phe molecules assume the structural

forms shown as species I-III in Fig. 1 . Similarly, the structural forms of the majority of Tyr molecules in solution with different pH values [$pK_1 = 2.20$, $pK_2 = 9.11$ and $pK_3 = 10.07$ (due to the side chain)] are shown as species I-IV in Fig. 1. In the sol, Ag particles are in the ionic Ag^+ state because of its low oxidation potential. The electrostatic interaction between the above species of amino acid molecules with positively charged Ag particles in solution, is responsible for the SERS effect. However, the structure of the molecules also plays an important role in determining the intensities of different SERS bands. Thus, a pH dependent study of SERS spectra with a comparison between the results for Phe and Tyr is expected to determine the metal-amino acid interaction and orientation of the adsorbed species on the metal surface.

The SERS spectra of Phe and Tyr adsorbed on Silver (Ag) colloids are available in the literature [3, 8]. We find that though the structure of these molecules are very similar (as mentioned above), their SERS spectra are widely different. To understand the interaction of these amino acids with Ag colloids we have studied the pH dependent optical absorption and SERS spectra of both Phe-Ag and Tyr-Ag complexes. From the relative change in intensities of the vibrational bands in SERS spectra we have compared the interaction, conformation and the orientation of these molecules on Ag particles. Section II covers the sample preparation techniques, which we have followed and other details regarding the instruments, which we have used for various measurements. In Section III, we have compared the possible surface geometry of the adsorbed Phe and Tyr on the surface of the Ag particles via pH dependent SERS measurements. Our conjecture from these experimental observations has been further supported by the surface geometry expected from the electrostatic interaction between Ag^+ and Phe or Tyr, obtained from the estimated atomic charge distribution at the different terminals of the amino acid molecules. In this section we have also shown the role of formation of hot sites to exhibit SERS spectra for metal-amino acid complex through simultaneous pH dependent optical absorption and SERS measurements. The interaction kinetics between the adsorbate and Ag colloids has been discussed in Section IV. Finally, in Section V we have summarized our results with a few concluding remarks.

II. MATERIALS AND METHODS

Silver nitrate (AgNO_3), sodium borohydride (NaBH_4), sodium hydroxide (NaOH), and hydrochloric acid (HCl) of analytical reagent grade (SRL, India), were used to prepare the Ag sol. Amino acids were also obtained from the above company. A colloidal silver solution was prepared in deionized water according to the method described by Creighton et al. [9]. This method essentially uses the reduction of 10^{-3} M AgNO_3 by an excess amount of 10^{-3} M NaBH_4 . 10^{-3} M AgNO_3 was added dropwise to 10^{-3} M NaBH_4 (placed in an ice bath under quick stirring condition) maintaining a 1:3 volume ratio. Stirring for 20 minutes was necessary to stabilize the colloidal solution. Later, it was left at room temperature for approximately 1 hour. The excess NaBH_4 evaporated and the remaining solution became transparent yellow in color. 10^{-3} M solution of Phe and Tyr were prepared in deionized water. The pH of the solution was adjusted by using 1 M HCl and 1 M NaOH . For SERS measurements Phe and Tyr solutions of different pH were added to the Ag sol. For all SERS experiments the volume ratio of Ag sol to amino acid solution was maintained at 9:1.

The SERS spectra were measured using a 488 nm Argon ion laser as an excitation source. The spectrometer is equipped with 1200 g/mm holographic grating, a holographic super-notch filter, and a Peltier cooled CCD detector. UV-Visible spectra were measured by Spectrascan UV 2600 (Chemito). All absorption spectra are recorded 2 minutes after addition of the amino acid to the sol. Samples for Transmission Electron Microscopy were deposited onto 300 mesh copper TEM grids coated with 50 nm carbon films. The excess water was allowed to evaporate in air. The grids were examined in JEOL 2010 microscope with Ultra-High Resolution (UHR) microscope using a LaB_6 filament operated at 200 kV.

The amino acid zwitterionic structures were drawn and energy minimized using SYBYL 6.92 (Tripos Inc., St. Louis USA). The structures were rendered in Pymol (Delano Scientific LLR, USA). The atomic charge distribution of the molecules has been estimated using the Gasteiger-Hückel method.

III. ADSORPTION OF PHENYLALANINE (PHE) AND TYROSINE (TYR) ON SILVER COLLOIDAL SURFACE: OPTICAL ABSORPTION AND SERS MEASUREMENTS

A. Phenylalanine (Phe) : Results and Discussion

The optical absorption spectra (OAS) of Phe at different pH in a colloidal solution of Ag are shown in Fig. 2. The Ag sol absorbs light at $\lambda_{max} = 392$ nm (A) [Fig. 2]. This band is associated with the dipolar surface plasmon of small, single, spherical particles of Ag. Transmission electron micrograph (TEM) of Ag sol shows formation of well-dispersed spherical Ag particles [Fig. 3(a)]. The average diameter of the Ag particles estimated from the λ_{max} in OAS in Fig. 2 and TEM image in Fig. 3(a) is ~ 90 Å.

Addition of Phe to the sol results in a decrease in intensity of peak A (due to a single silver particle), along with an appearance of a new band at around 561 nm (B) due to aggregated Ag particles. In Fig. 2 we have shown the change in the optical absorption spectrum of Ag sol with addition of Phe of pH varying from 1.5 to 12.5. The change in the ratio of intensity of peak B to that of peak A with variation in pH is shown in Fig. 4. The nature of aggregation of the silver particles, with addition of Phe of different pH, as obtained from TEM images, is shown in Fig. 3(b) to Fig. 3(d). Addition of Phe at a very low pH (below pH 2) to the Ag sol results in an immediate agglomeration and precipitation of Ag particles (not shown in the figure). One may also note the green curve in Fig. 2, where any signature of colloidal Ag particle is nearly absent. Between pH 2 and pH 3.5 the metal particles agglomerate appreciably. However, they are not big enough to precipitate immediately [Fig. 3(b) for pH 2]. For Phe with medium pH in Ag sol, one observes clustering of Ag particles in solution without much agglomeration or precipitation [Fig. 3(c) for pH 8 of Phe]. Addition of Phe at very high pH values (above 9) prohibits the clustering of Ag particles, which now spread out in solution [Fig. 3(d)].

In Fig. 5 we have shown the Raman spectrum of an aqueous Phe solution of 0.5 M (mentioned as Phe-C in the rest of the article) at pH 6.5 within the spectral window of 500- 3200 cm^{-1} (after subtracting the broad background of water in the range 1500-1800 cm^{-1} and 2800-3200 cm^{-1}). The assignments of bands in Phe-C, summarized in Table I, are based on the available Raman data for Phe [10, 11]. The most intense band at 1008

TABLE I: Assignment of vibrational bands for Phe-C (Raman spectrum) and Phe-Ag complex(SERS spectra)

Assignment	Phe - C (cm $^{-1}$)	SERS Phe (cm $^{-1}$)
Benzene ring breathing mode (ν_1)	1008	1000
COO $^-$ rocking, wagging, bending	500-700	500-700
ν_{C-C} of Benzene ring	901	-
C-H vibration in benzene ring	3080	3065
C-COO $^-$	929	936
CN	1036	1035
NH $_3^+$	1595	1582
CH	1251	1235
CH	2976	2915
COO $^-$	1413	1375
CH $_2$ wagging	1332	-
CH $_2$ deformation	1400	-

cm^{-1} has been assigned to the benzene ring breathing mode (ν_1). Other less intense but prominent bands appear at 901 cm^{-1} , 929 cm^{-1} , 1036 cm^{-1} , and 1595 cm^{-1} due to ν_{C-C} , C-COO $^-$, CN and NH $_3^+$ vibrations, respectively. The bands belonging to ν_{CH} , ν_{C00^-} , CH $_2$ wagging, CH $_2$ deformation are weak and observed at 2976 (also at 1251), 1413, 1332 and 1400 cm^{-1} , respectively. COO $^-$ rocking, wagging, and bending modes appear between 500 and 700 cm^{-1} . The feature at 3080 is due to the breathing motion of the hydrogen atoms in the benzene ring (C-H vibration).

SERS spectra (solid lines) of $1 \times 10^{-3} \text{ M}$ Phe, 2-3 orders of magnitude more dilute than the concentration typically required for nonresonance Raman scattering, with pH from 1.5 to 12.5 are shown in Fig. 6. We have recorded spectra of Phe-Ag complexes by changing the pH values by 1.0 unit over this range. However, in Fig. 6, we have shown a few characteristic spectra. SERS peak positions are also listed in Table 1. The Raman spectrum of aqueous Phe solution with the low concentration (0.001 M) at pH 7 is shown by the dotted line in the same figure.

To understand the interaction of the adsorbed species on the surface of Ag particles, we

will make use of both SERS and absorption spectra. It is clear from Fig. 5 and Fig. 6 that intensities of the above mentioned vibrational modes change in SERS spectra with variation in pH. It is also interesting to note that below the pH value of 4.5 and above the pH value of 10 the SERS spectrum is extremely weak for the complex. As we mentioned before, upon addition of Phe of very low pH (below 3.5, value of $pK_1 = 2.58$) the Ag particles agglomerate and then precipitate or form bigger particles [see Fig. 2 green curve and also Fig. 3 (b)]. The high pH value (above 9.5, $pK_2 = 9.24$) results in a spreading of Ag particles, as shown in Fig. 3(d). The slight red shifted broad navy blue spectrum for pH 12 in Fig. 2 indicates the absence of agglomerated Ag particles alone in the sol. Under both these conditions the number of hot sites decreases in solution, which in turn results in a decrease in the intensity of the SERS spectrum. In other words, the inefficient SERS is related to the failure of colloid activation due to insufficient complexation of Phe to the Ag surface. Intensities of the vibrational bands in SERS spectra are quite prominent, though of varying intensities, for the pH values ranging from 4.5 to 9.5. Thus, from Fig. 3 and Fig. 4, we conclude that for efficient SERS the aggregation of Ag colloidal particles (Intensity ratio of B to A in optical absorption spectra) plays an important role via the formation of hot sites.

The SERS spectra at pH below 3.5, between 3.5 and 9.5, and above 9.5 should correspond to species I, II and III respectively, shown in Fig. 1(a). For Benzene molecule [2] SERS surface selection rule states that vibrational bands which draw the intensity of Raman polarizability component α_{zz} is most intense, where z is the surface normal. If a benzene molecule is absorbed, such that the ring lies parallel to the metal surface, α_{zz} contributes only to its two A_{1g} modes ν_1 (at 992 cm^{-1}) and ν_2 (at 3056 cm^{-1}). The maximum contribution to the α_{zz} component of the polarizability of benzene comes from the π - electrons. Thus, ν_1 , which perturbs the carbon ring directly, plays a more prominent role in affecting α_{zz} than ν_2 , which involves only hydrogen atoms [2]. However, if the benzene ring is perpendicular to the metal surface rather than lying parallel, one expects ν_2 would be more intense than ν_1 . In aqueous Phe these two peaks of the aromatic ring structure appear at 1008 and 3080 cm^{-1} . In SERS spectra these modes are obtained at 1000 and 3065 cm^{-1} . Above the pH value 3.5, the intensity of the band at 1000 cm^{-1} increases with increase in pH of Phe till the pH value reaches 9.5. Beyond this value of pH the 1000 cm^{-1} band disappears [Fig. 7a]. The low intensity ratio of the band at 1000 cm^{-1} and 3056 cm^{-1} compared to what we observe for Phe-C (Fig. 5) indicates that the aromatic ring of Phe is absorbed *nearly*

parallel to the surface of the Ag colloids. With increase in pH there is a conformational change in the molecule; the attached molecule tilts more and more towards the surface (flatter) as indicated by the increase in ratio of $I(\nu_1)/I(\nu_2)$, shown in Fig. 7(b). The above intensity variation and shift in the frequency of these bands in the SERS spectrum with respect to their frequencies in the spectrum of the solution, indicate that the π -system of Phe participates in complex formation with Ag.

In Fig. 6, a relatively strong band at 1375 cm^{-1} beyond pH value 3.5 (note that $\text{pK}_1 = 2.58$ for Phe) and the variation in intensity of this band with pH indicates that the carboxylic group, $-\text{COO}^-$, upon deprotonation is clearly absorbed on the surface of the Ag colloids [Fig. 8(a)]. There are several weak bands between 500 and 750 cm^{-1} due to different COO^- vibrational modes. In SERS spectra of Phe-Ag the CH - stretching vibration appears at 2915 cm^{-1} . The νCH_2 vibrational modes are absent in SERS spectra, indicating that the methylene group is relatively far from the Ag surface. Though, it is not expected that the NH_3^+ group be directly attached to Ag^+ colloids in the sol, the relatively strong band due to asymmetrical deformation of NH_3^+ at 1582 cm^{-1} indicates that amine group of the molecule stays relatively close to the Ag surface. The intensity of this band drops down with increase in pH as NH_3^+ transforms to NH_2 [Fig. 8(b)]. The relatively strong band due to νCN at 1036 cm^{-1} , and its increase in intensity with increase in pH [Fig. 8(c)] can be explained by assuming the proximity of amine group to the silver surface.

B. Tyrosine (Tyr) : Results and Discussion

The optical absorption spectra of Tyr at different pH in colloidal solution of Ag are shown in Fig. 9. As observed in case of Phe [Fig. 2], the addition of Tyr to the sol results in the appearance of a new band at around 520 nm (B1) due to aggregation of Ag sol along with a decrease in intensity of peak A (due to a single particle). The variation in the ratio of the intensity of peak B1 to that of peak A with change in pH is shown in Fig. 10. The nature of aggregation of the silver particles with addition of Tyr of different pH, as obtained from TEM images are shown in Fig. 11 (a) - Fig. 11(c).

In Fig. 12 we have shown the Raman spectrum of an aqueous Tyr solution of 0.5 M (Tyr-C) at pH 6.0 (after subtracting the luminescence background). The assignment of vibrational bands in Tyr-C has been summarized in Table II. The most intense band at 828

cm^{-1} has been assigned to the breathing mode of the aromatic ring structure of Tyr [8]. Other less intense but prominent bands, appear at 931 cm^{-1} , 1304 cm^{-1} and 2967 cm^{-1} , are due to $\text{C}-\text{COO}^-$, CH_2 wagging and CH vibrations, respectively. The bands belonging to ν_{CH} vibrations in the ring appears at 3061 cm^{-1} .

TABLE II: Assignment of vibrational bands for Tyr-C (Raman spectrum))

Assignment	Tyr - C (cm^{-1})
Ring breathing mode	828
$\text{C}-\text{COO}^-$	931
CH_2 wagging	1304
CH	2967
CH vib. in ring	3061

The SERS spectra of Tyr ($1 \times 10^{-3} \text{ M}$) with pH 1.5 to 12.5 are shown in Fig. 13. Raman spectrum of aqueous Tyr solution of same concentration at pH 7 is shown by a dotted line in the same figure. It is interesting to note that though the molecular structure of Tyr is similar to that of Phe except for an -OH group in the para position of the aromatic ring, the SERS spectrum is entirely different from that of Phe. In aqueous solution, Tyr becomes Tyrosinate, TyrO^- , at pH of 10.07 (pK_3). However, Tyr deprotonates upon adsorption, ie. they are absorbed as TyrO^- on metal surface (It has been shown that SERS spectra of Tyr-Ag should cover much narrower spectral region) [3, 8]. We assign the broad and unresolved band between 1200 and 1500 cm^{-1} in Fig. 13, measured with long integration time (5 minutes as in our case) for the range of pH value from 3.5 to 9.5, to temporal averaging (averaging of strongly fluctuating contribution to overall intensity profile) of Tyr SERS spectrum. The reason is the following : In addition to the direct coordination of the aromatic ring with Ag^+ , TyrO^- can be adsorbed on the Ag surface either via the carboxylic acid group or via both the amino and carboxylic group or via the phenol hydroxyl group. The ensemble average of all these complexations results in a broad band. This has been also been shown from quantum chemical estimates of vibrational energies using Hartree-Fock self-consistent field molecular orbital calculation for TyrO^- -Ag complex [3]. In Fig. 14 we have shown the variation in the intensity of the peak at 1390 cm^{-1} with the pH of the Tyr solution. In the acidic region ($\text{pH} < 4.5$) an extensive aggregation [Fig. 11(a)] of the colloid

silver leads to a complete loss of the SERS signal. The decrease in SERS spectral intensity for higher pH at 10.5 and above is due to spreading out of the Ag particles in sol, which decreases the number of hot sites necessary for SERS [Fig 11 (c)]. Following the discussion on Phe-Ag complex, the role of agglomeration of Ag particles (formation of the number of hot sites in metal sol) to exhibit efficient SERS of Tyr-Ag complex is also clear from the variation in intensity ratio of peak A and peak B1 with pH in absorption spectra as shown in Fig. 10 and also from the TEM images shown in Fig. 11.

C. Comparison of interaction in Phe-Ag and Tyr-Ag complex

From the above experimental results and the corresponding discussion we observe that the Phe and Tyr molecules behave very differently while forming complexes with Ag molecules. For Phe the aromatic ring lies nearly flat on Ag surface. Both carboxylic and amine groups are important in adsorption of Phe on metal particles; whereas, the methylene (CH_2) group is relatively inert. This signifies that the aromatic ring, carboxylic and amine group of Phe lie in close proximity of metal particles, whereas the methylene group stays away. On the other hand, Tyr adsorbs on Ag surface as Tyrosinate. At any instant of time, interaction of metal ion either with carboxylic group or with amine group or with oxygen in the side chain can be more probable than the other two interactions.

To support our above conjecture, we have looked into the atomic charge distribution at the different terminals of Phe and Tyr molecules in the energy minimized zwitterionic forms (which bind with Ag ion to form a complex), shown in Fig. 15 (a) and 15(b). From the hybrid density functional theory, it has been shown that while forming a complex with Phe or Tyr, the Ag^+ preferentially occupies the cavity formed in the molecular structure, shown in Fig. 15 [13]. If one takes into account only the electrostatic affinity between Ag and Phe/Tyr molecule, from the atomic charge distribution, shown in Fig. 15, it appears that the following interactions are possible for both Ag-Phe or Ag-Tyr complexes - (a) it is unlikely for the NH_3^+ group to be directly attached with the positively charged Ag surface, though it is in close proximity of the Ag^+ , (b) the CH_2 group is away from Ag^+ , which results in a weak electrostatic interaction between them, (c) the negative charge distribution on oxygen atoms of the carboxylic acid group and ring structure indicate the possibility of a strong electrostatic interaction with the positive metal ion (d) the aromatic ring is parallel to the

surface of the Ag^+ . From a more careful analysis we see that in Phe the charges on the oxygen atoms of the carboxylic group are - 0.56 units, whereas, those on Tyr are - 0.29 and - 0.36 units. The side chain oxygen atom of Tyr has a charge of - 0.34 units. We believe the relatively large negative charge on oxygen terminals in Phe holds the positive metal ion firm in its position via Coulombic interactions. However, the relatively less negative charge at the carboxylic oxygen terminals and at the side chain result in a smeared position of the Ag^+ in the Tyr cavity [Fig. 15 (b)] compared to what we observe in case of the Phe-Ag complex [Fig. 15 (a)]. This explains the weak and broad SERS band for Tyr-Ag complex. It is also interesting to note that except in these terminals, the charge distributions are nearly the same on all other atoms in Phe and Tyr.

IV. KINETIC MEASUREMENTS ON AG-PHE AND AG-TYR INTERACTION

We have seen in the previous section that the formation of hot sites due to the optimum agglomeration of Ag colloidal particles plays a direct role to form stable Ag-ligand complex. In this section, we have confirmed the same fact by measuring the interaction kinetics of Phe-Ag and Tyr-Ag complexes by SERS and absorption measurements. To study the kinetics of the interaction we have recorded the intensity of optical absorption peak at 535 nm (peak B due to agglomerated Ag in Fig. 2) for Phe-Ag complex and 490 nm (peak B1 in Fig. 9) for Tyr-Ag complex with time. The variations in intensities of these two peaks with time are shown in Fig. 16 (a) and 16 (b), respectively. We clearly observe two different decay rates for both the peaks. For the first 120 sec the decay process is very fast compared to what is observed later. The decay time constants are 58 (τ_1) sec and 178 (τ_2) sec for Phe and 63 (τ_1) sec and 100 (τ_2) sec for Tyr.

To correlate the optical absorption and SERS measurements, we studied the kinetics of SERS spectra of 5×10^{-3} M ligand- Ag mixture at pH 8 (about which we get maximum SERS intensity for the most intense peaks). Each spectrum was taken for 2 minutes with 1 minute interval. The exponential drop in intensities of the strongest band at 1000 cm^{-1} for Phe and the band at 1392 cm^{-1} in Tyr are shown in Fig. 17(a) and 17(b). The decay constants are estimated to be 213 sec and 113 sec, respectively. These values of the time constants match reasonably well with the values of τ_2 , which we have obtained from optical absorption measurements. Thus, we confirm that the metal-amino acid interaction is directly

related to the aggregation of the Ag colloids. Here we would like to mention that because of experimental limitations the absorption spectra in Fig. 2 and Fig. 10 or SERS spectra in Fig. 6 and Fig. 14 are recorded 2 minutes after addition of amino acids in Ag sol. Thus, the effect of initial kinetics of interaction, at time scale τ_1 , is not observed in these spectra.

However, a careful observation of the initial change in colour of the sol with addition of amino acid indicates fast kinetics of the interaction between ligand molecules and Ag sol. The as-prepared Ag sol is yellow in colour and is stable for more than 24 hrs at 4 °C. The agglomeration of the particle after addition of amino acids changes the colour from yellow to pink to blood red as shown in Fig. 18 (a) for Phe and yellow to amber to olive green as shown in Fig. 18 (b) for Tyr. It is to be noted that the change in colouration of the solution is rapid (distinct by naked eye) for first ~ 60 seconds for both Phe-Ag and Tyr-Ag. This time scale matches with value of τ_1 obtained from kinetic studies by absorption measurements. This initial change in color may be due to the increase in the size of the particles from single particle to doublets, triplets and higher multiplets. Gradually, with time, the colour of the solution fades out indicating the breakdown of agglomerated particles into smaller fragments.

V. SUMMARY

Though structurally close, Phe and Tyr, behave very differently, when they form complexes with Ag colloids. To understand this difference, we have compared the metal-amino acid interaction in Phe-Ag and Tyr-Ag complexes by pH dependent SERS measurements. From the intensity variations of the vibrational bands in SERS spectra with the pH of the adsorbates, we have proposed the relative orientation and interaction of the adsorbed molecules on the Ag surface. We have addressed a long standing query, as to whether the amine group is directly attached with Ag surface along with carboxylate group in these systems. Using Gasteiger-Hückel method to estimate the atomic charge distribution at different terminals of the zwitterionic amino acid molecules, we have noted that, though the structures of Phe and Tyr are quite similar, (except an -OH group at the para position of the ring in the latter), the atomic charge distributions at the oxygen sites of these molecules, are quite different. If we assume only the electrostatic interaction between different terminals of the adsorbates with Ag^+ , the above charge distribution confirms the interaction and orientation of the amino

acid molecules in the complexes, which we have proposed from SERS measurements.

In addition, the appearance of SERS bands have been explained with the help of pH dependent TEM and optical absorption measurements. We have seen that formation of hot sites via optimum aggregation of Ag particles induced by Phe/Tyr results in an increase in intensity of the optical absorption band of the Ag aggregates and, concurrently, an increase in SERS band intensities. We have also shown that the state of aggregation is a key parameter in SERS. We have discussed the reaction kinetics of this interaction process using spectroscopic measurements.

VI. ACKNOWLEDGEMENTS

Authors thank P.V. Satyam and J. Ghatak, IOP, Bhubaneshwar, India, for their assistance in the TEM work. AR thanks Department of Science and Technology, India, and Third World Academy of Science, ICTP, Italy for financial assistance.

- [1] Shoeib, T., A. Cunje, A. C. Hopkinson, and K. W. Michkael Siu. 2002. Gas-phase fragmentation of the Ag⁺ -Phenylalanine complex : Cation - interactions and radical cation formation. *J. Am. Soc. Mass Spectron.* 13:408-416.
- [2] Suh, J.S., and M. Moskovits. (1986). Surface-enhanced Raman spectroscopy of amino acids and nucleotide bases adsorbed on silver. *J. Am. Chem. Soc.* 108:4711-4718.
- [3] Bjerneld, E.J., P. Johansson, and M. Kall. 2000. Single molecule vibrational fine-structure of Tyrosine adsorbed on Ag nanocrystals. *Single Mol.* 3:239-248.
- [4] Bjerneld, E.J., F. Svedberg, P. Johansson, and M. Kall. 2004. Direct observation of heterogeneous photochemistry on aggregated Ag nanocrystals using Raman spectroscopy : The case of photoinduced degradation of aromatic amino acids. *J. Phys. Chem. A* 108:4187-4193.
- [5] Curley, D. and O. Siiman. 1988. Conformation and orientaion of the Haptens, 2,4-Dinitropheyl amino acids, on colloidal silver from surface-enhanced Raman scattering. *Langmuir.* 4:1021-1032.
- [6] Kneipp, K., H. Kneipp, I. Itzkan, R. R. Dasari, and M. S. Feld. 1999. Ultrasensitive chemical analysis by Raman spectroscopy. *Chem. Rev.* 99:2957-2975.

- [7] Teiten, B., and A. Burneau. 1997. Detection and sorption study of Dioxouranium (VI) ions on N-(2-Marcaptopropionyl) glycine-modified silver colloid by Surface enhanced Raman scattering. *Journal of Raman spectroscopy*. 28:879-884.
- [8] Rava, R.P., and T. G. Spiro. 1984. Selective enhancement of Tyrosine and Tryptophan resonance Raman spectra via ultraviolet laser excitation. *J. Am. Chem. Soc.* 106:4062-4064.
- [9] Creighton, J., C. Blatchford, and M. Albrecht. 1979. *J. Chem. Soc. Faraday Trans.* 75:790.
- [10] Fodor, S.P.A., R.A. Copeland, C.A. Grygon and T.G. Spiro. 1989. Deep-ultraviolet Raman excitation profiles and vibronic scattering mechanisms of phenylalanine, tyrosine and tryptophan. *J. Am. Chem. Soc.* 111:5509-5518.
- [11] Rava, R.P., and T. G. Spiro. 1985. Resonance enhancement in the ultraviolet Raman spectra of aromatic amino acid. *J. Phys. Chem.* 89:1856-1861.
- [12] Herne, T.M., A. M. Ahern, and R. L. Garrell. 1991. Surface Enhanced Raman spectroscopy of peptides : Preferential N-terminal adsorption on colloidal silver. *J. Am. Chem. Soc.* 113:846.
- [13] Shoeib, T., K.W. Michael Siu, and A.C. Hopkinson. 2002. Silver ion binding energies of amino acids : Use of theory to assess the validity of experimental silver ion basicities obtained from the kinetic method. *J. Phys. Chem.* 106:6121-6128.

Figure Captions

Figure 1. Different ionic species of Phe and Tyr at different pH values

Figure 2. Absorption spectra of Phe -Ag mixture at different pH values.

Figure 3. Transmission electron micrograph of (a) Ag sol and Phe-Ag mixture at (b) pH 2 (c) pH 8, and (d) pH 11.

Figure 4. Variation of intensity ratio of peak B to peak A in optical absorption spectra for Phe-Ag complex.

Figure 5. Raman spectrum of Phe in solution at concentration 0.5M.

Figure 6. Raman spectrum (dotted) of Phe and SERS spectra (solid lines) of Phe-Ag complex (1×10^{-3} M) at different pH of Phe.

Figure 7. Intensity variation of SERS bands at (a) 1000 cm^{-1} , (b) intensity ratio $I(\nu_1)/I(\nu_2)$ with pH variation from 1.5 to 12.5 for Phe-Ag complex.

Figure 8. Intensity variation of SERS bands at (a) 1375 cm^{-1} , (b) 1582 cm^{-1} and (c) 1036 cm^{-1} with pH variation from 1.5 to 12.5 for Phe-Ag complex.

Figure 9. Absorption spectra of Tyr -Ag mixture at different pH.

Figure 10. Variation of intensity ratio of peak A and peak B1 in optical absorption spectra for Tyr-Ag complex.

Figure 11. Transmission electron micrograph of Tyr-Ag mixture at (a)pH 2, (b) pH 7.5, and (c) pH 11.

Figure 12. Raman spectrum of Tyr in solution at concentration 0.5M.

Figure 13. Raman spectrum of Tyr (dotted) and SERS spectra (solid lines) of Tyr-Ag complex (1×10^{-3} M) at different pH.

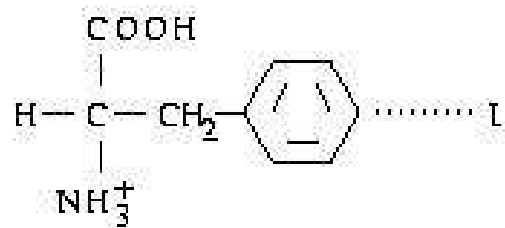
Figure 14. Intensity variation of Raman bands at 1390 cm^{-1} in Tyr with change in pH from 1.5 to 12.5.

Figure 15. Atomic charge distribution on (a) Phe and (b) Tyrosinate, obtained by Gasteiger-Hückel method.

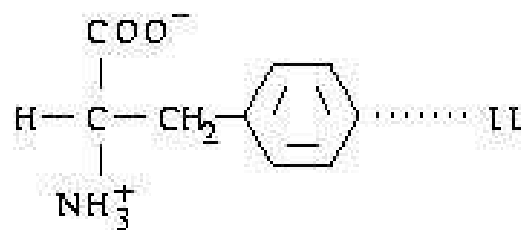
Figure 16. Kinetic study of (a) the feature at 535 nm in optical absorption spectra of Phe -Ag mixture and (b) the feature at 490 for Tyr-Ag complex. Insets of the figures show same for first 2 min. duration

Figure 17. Kinetic study of the most intense peak in SERS spectra for (a)Phe-Ag complex and (b) Tyr-Ag complex.

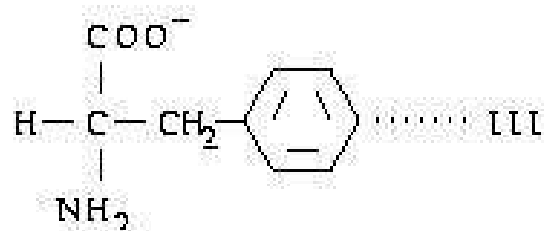
Figure 18. Change in colour of (a) Phe-Ag complex and (b) Tyr-Ag complex with time



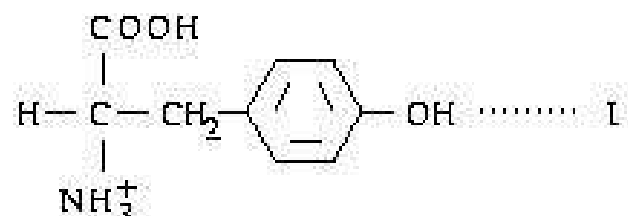
Below pK_1



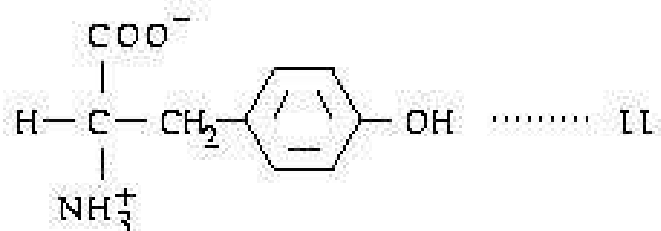
Between pK_1 and pK_2



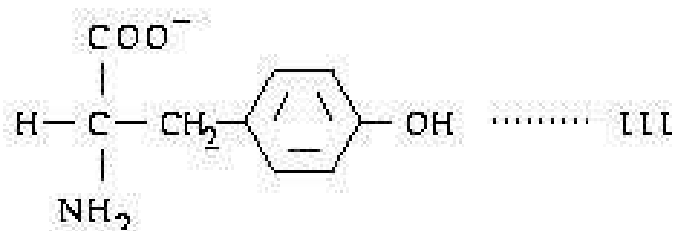
Above pK_2



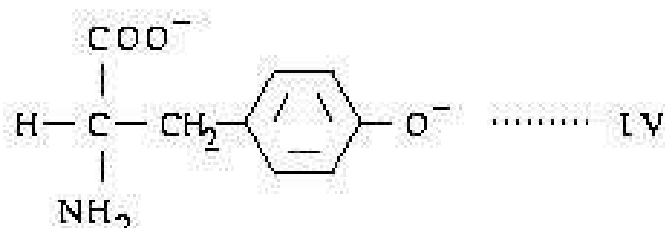
Below pK_1



Between pK_1 and pK_2



Between pK_1 and pK_3



Above pK_3

Phenylalanine

Tyrosine

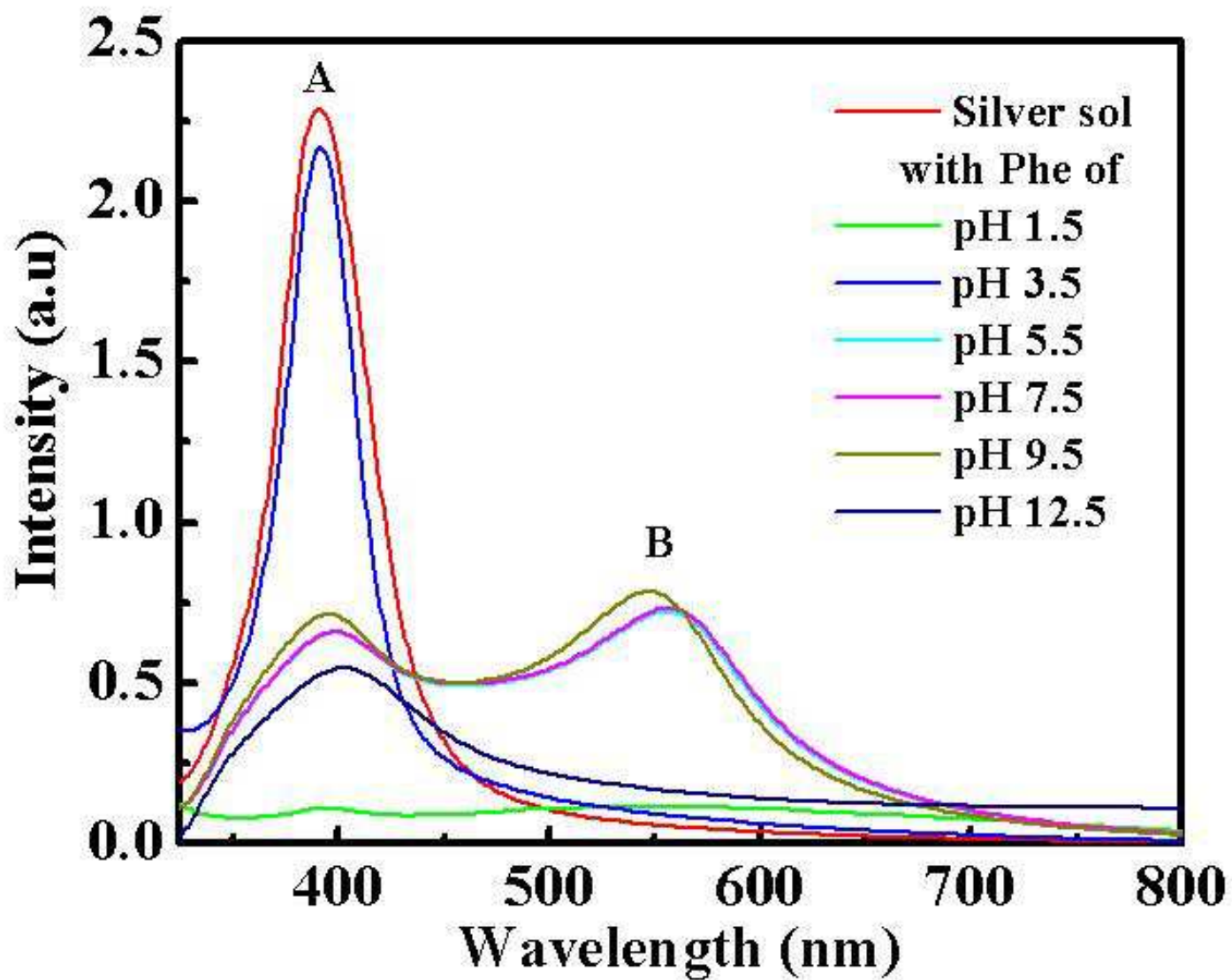


Figure 2. Singha et al

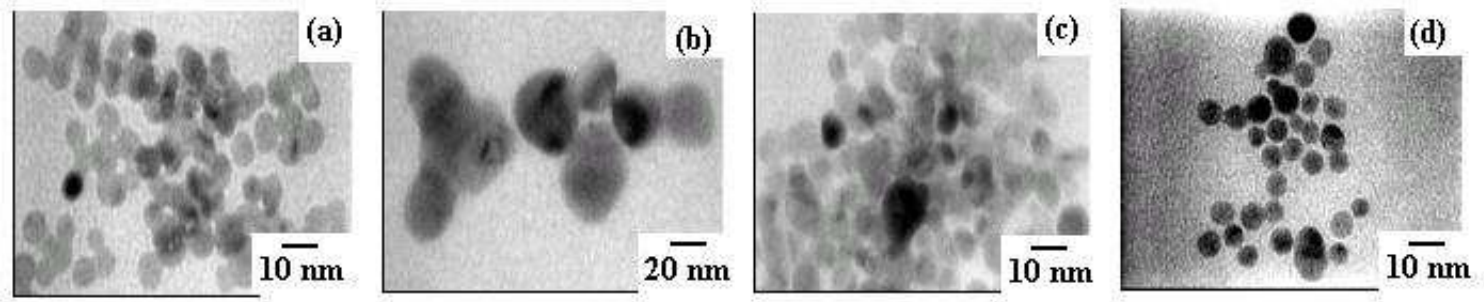


Figure 3. Singha et a

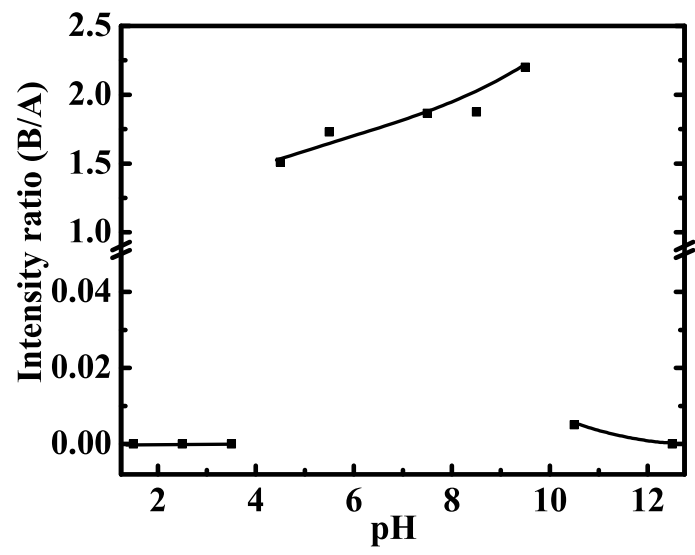


Figure 4. Singha et al

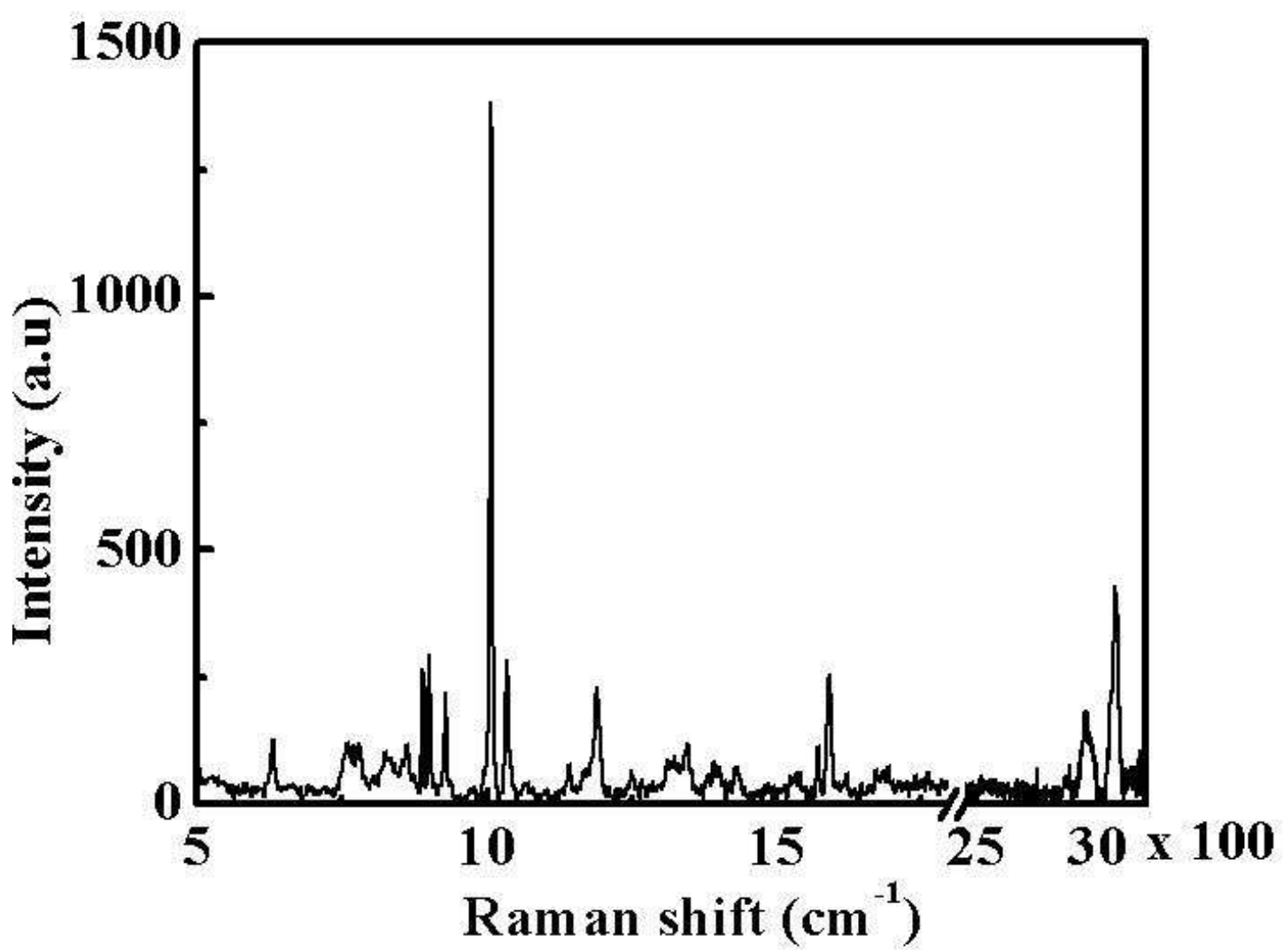


Figure 5. Singha et al

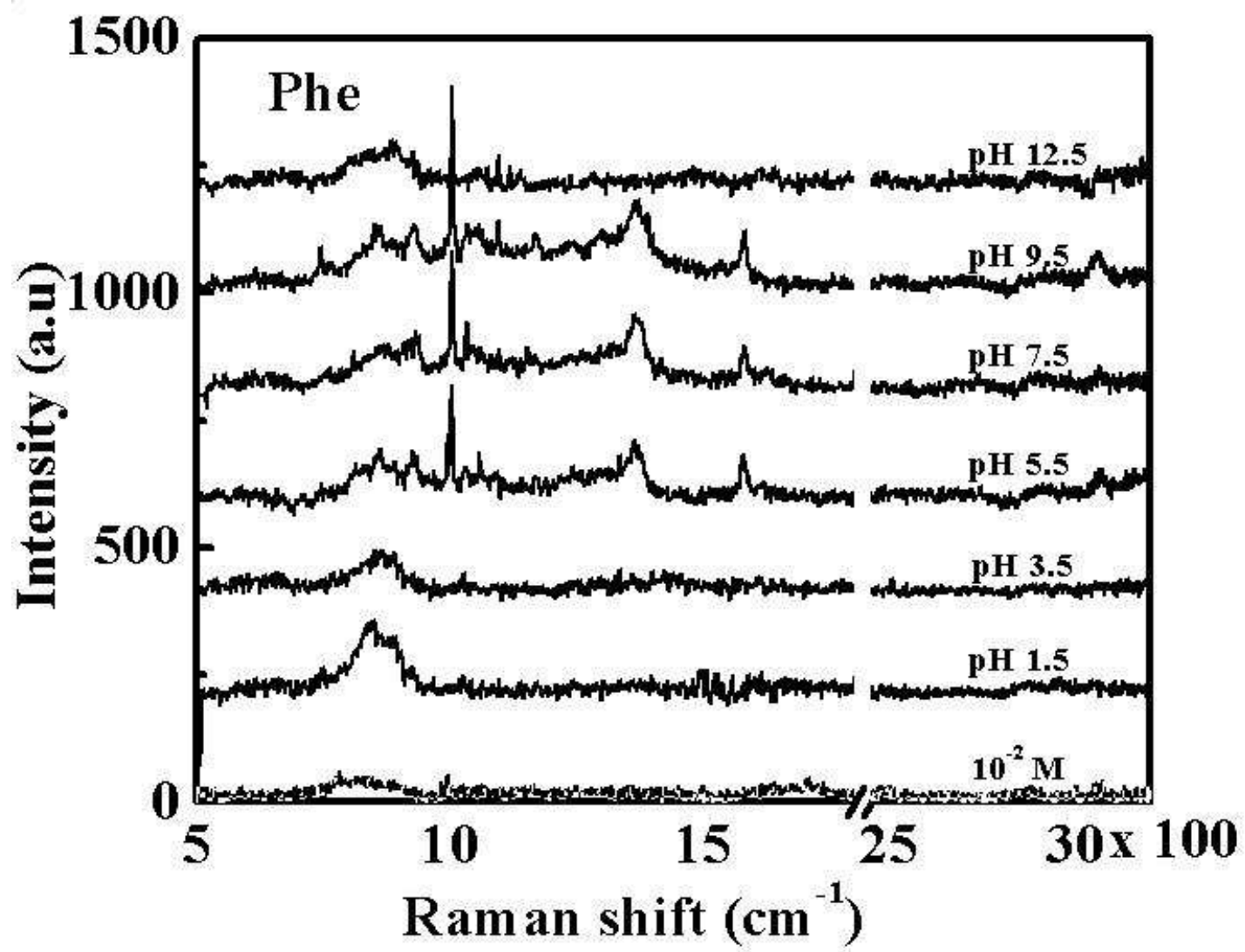


Figure 6. Singha et al

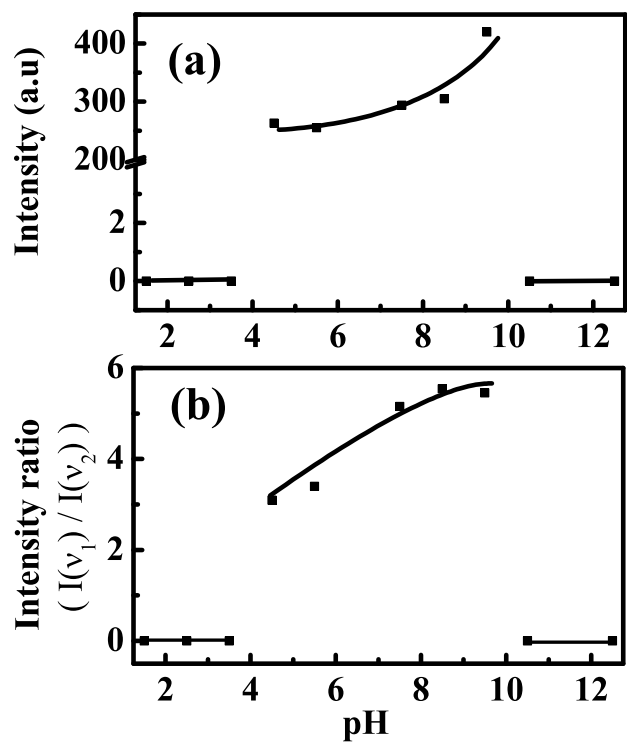


Figure 7. Singha et al

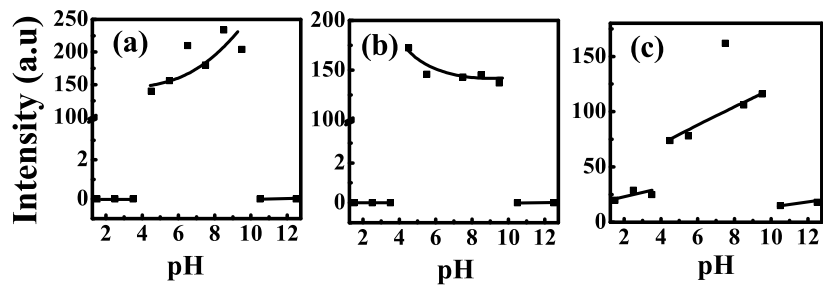


Figure 8. Singha et al

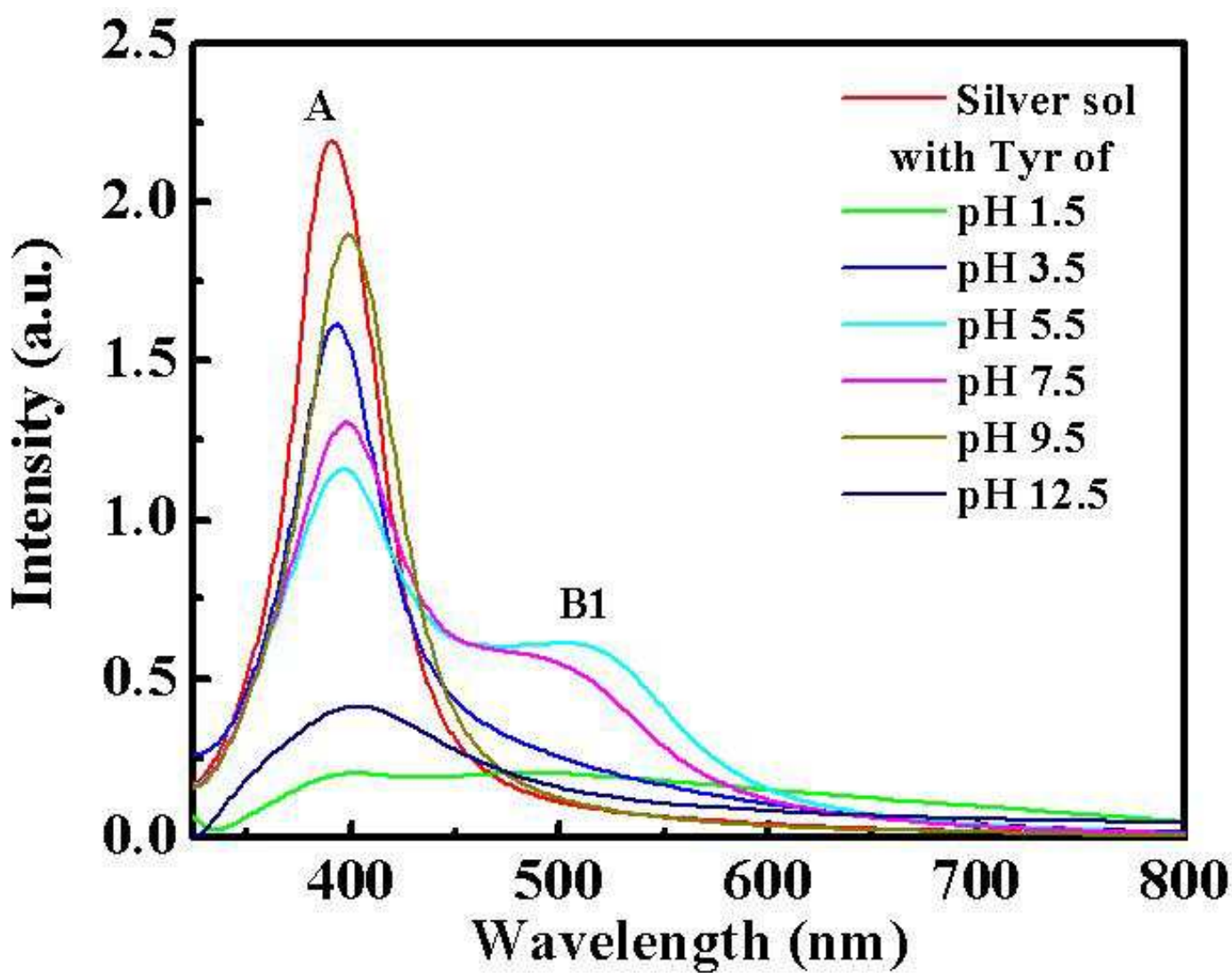


Figure 9. Singha et al

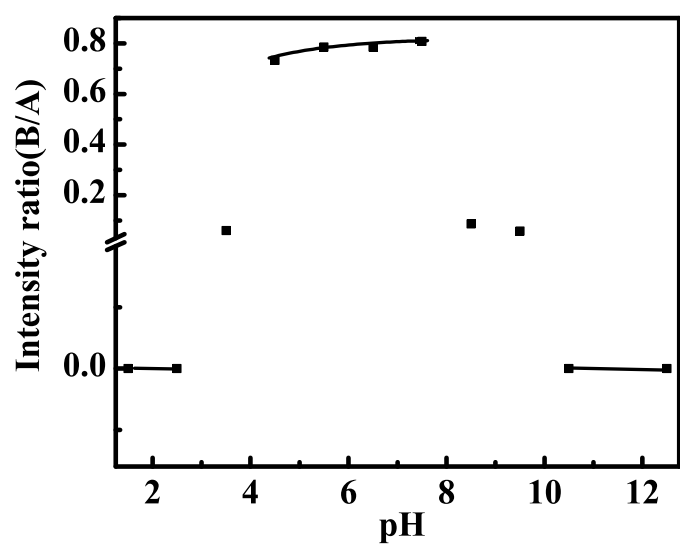


Figure 10 Singha et al

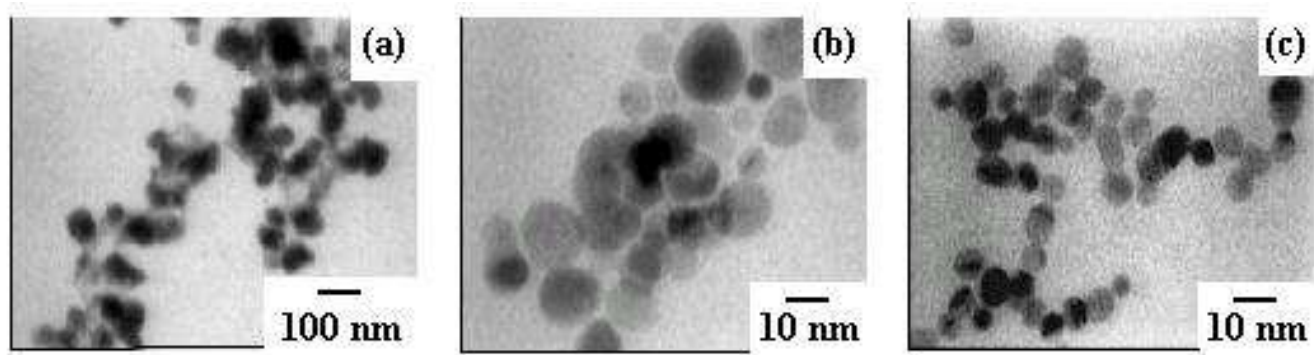


Figure 11. Singha et al

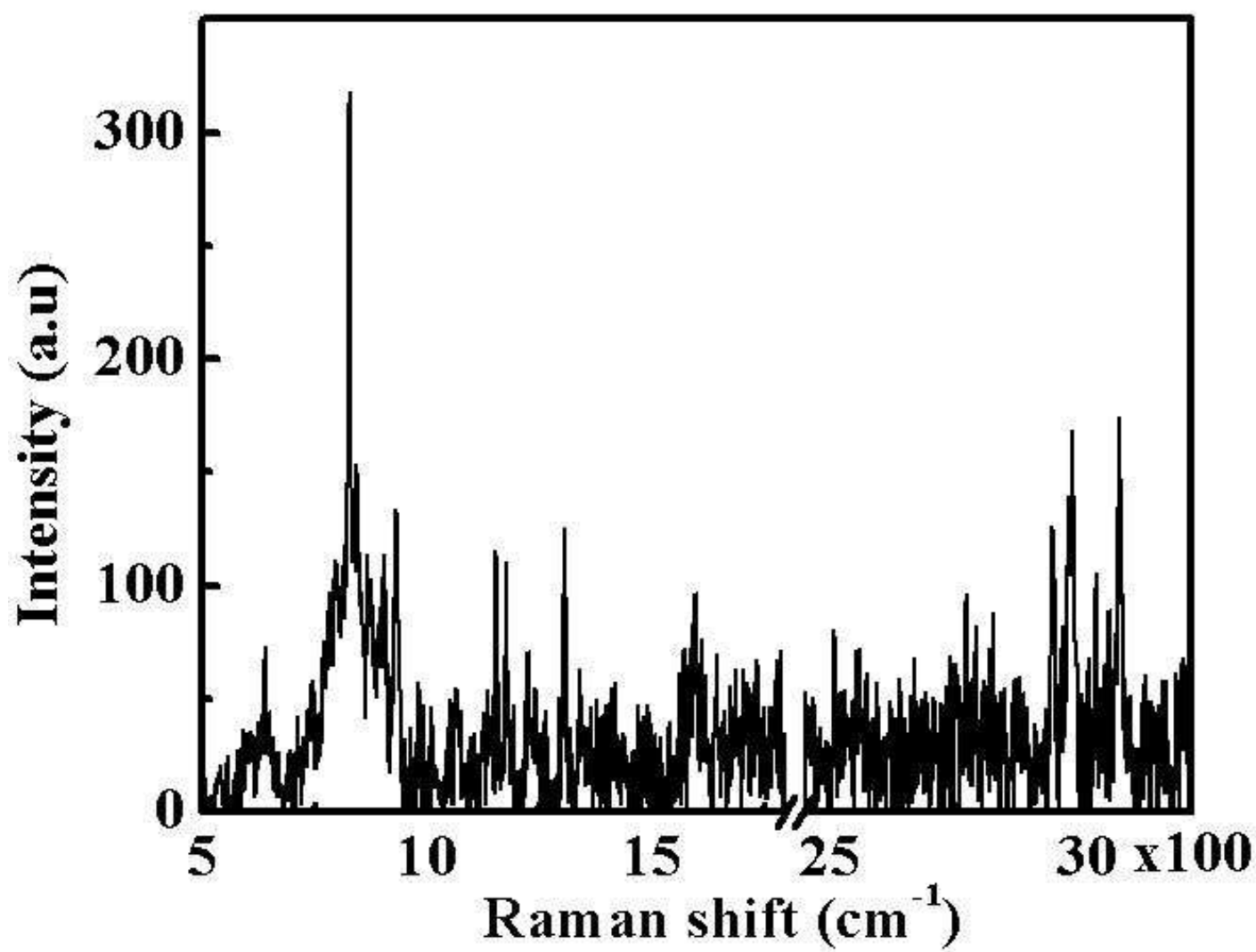


Figure 12. Singha et al

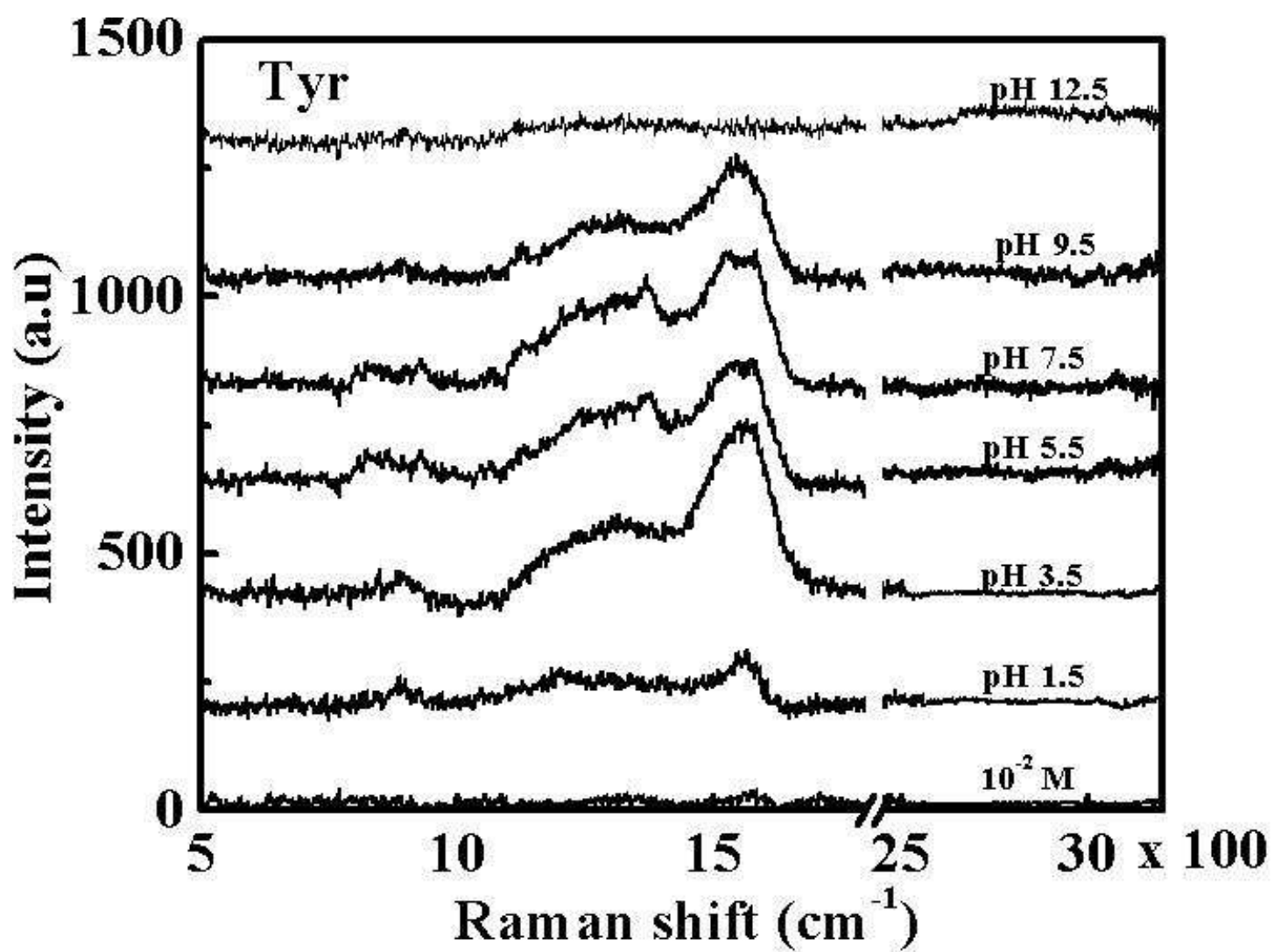


Figure 13. Singha et al

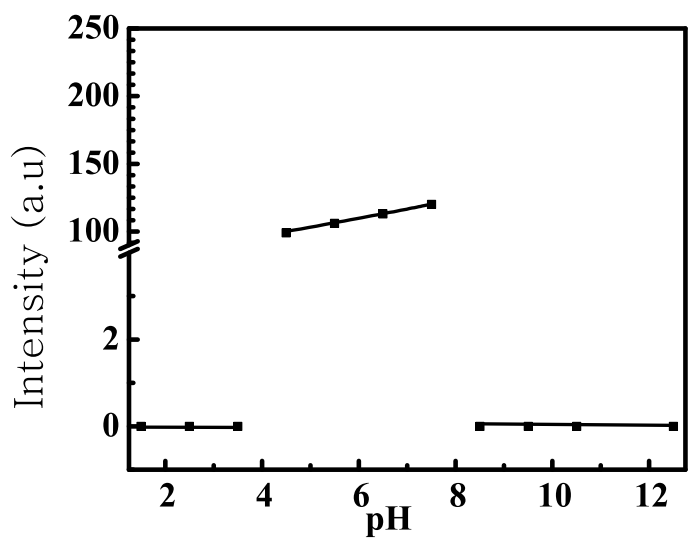


Figure 14. Singha et al

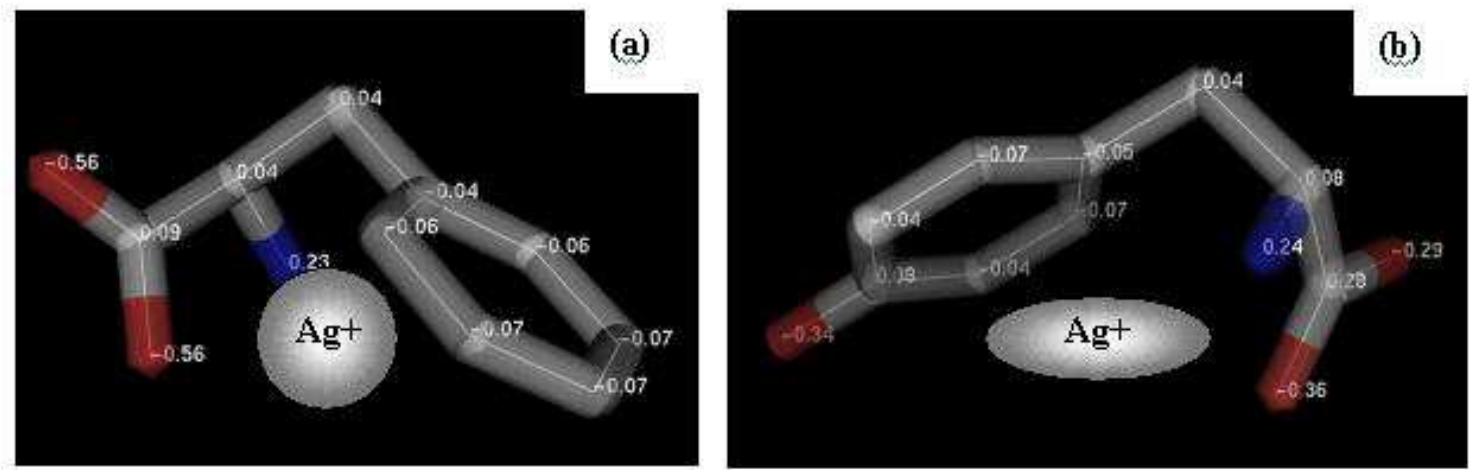


Figure 15. Singha et al

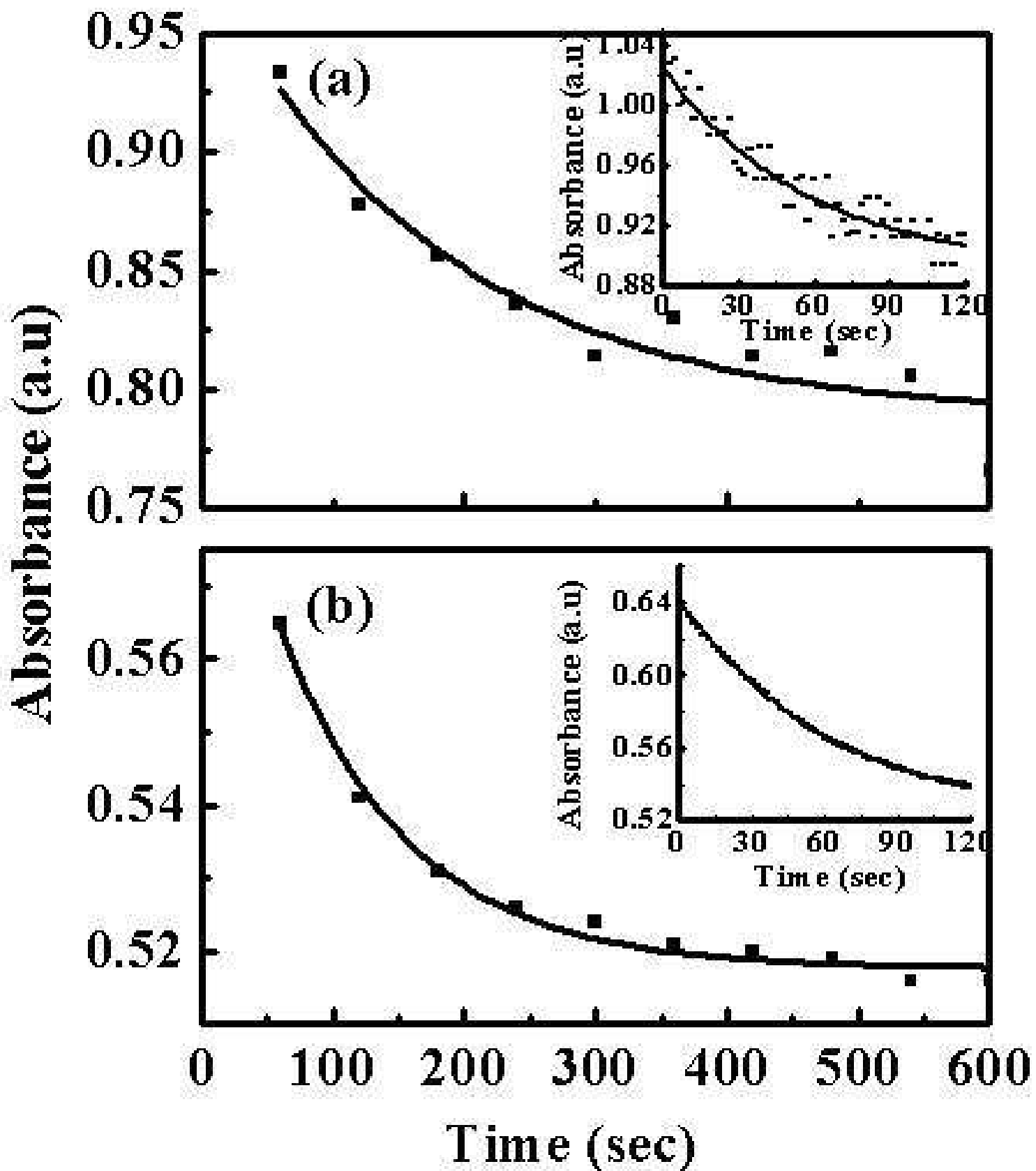


Figure 16. Singha et al

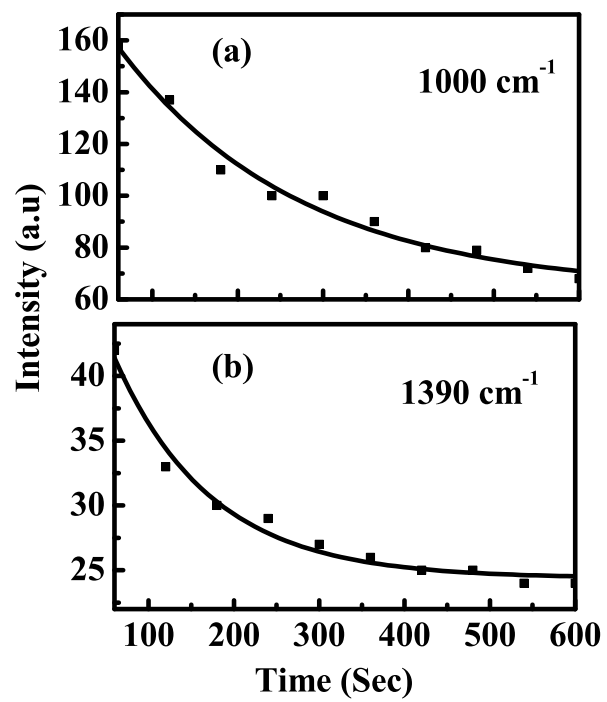


Figure 17. Singha et al

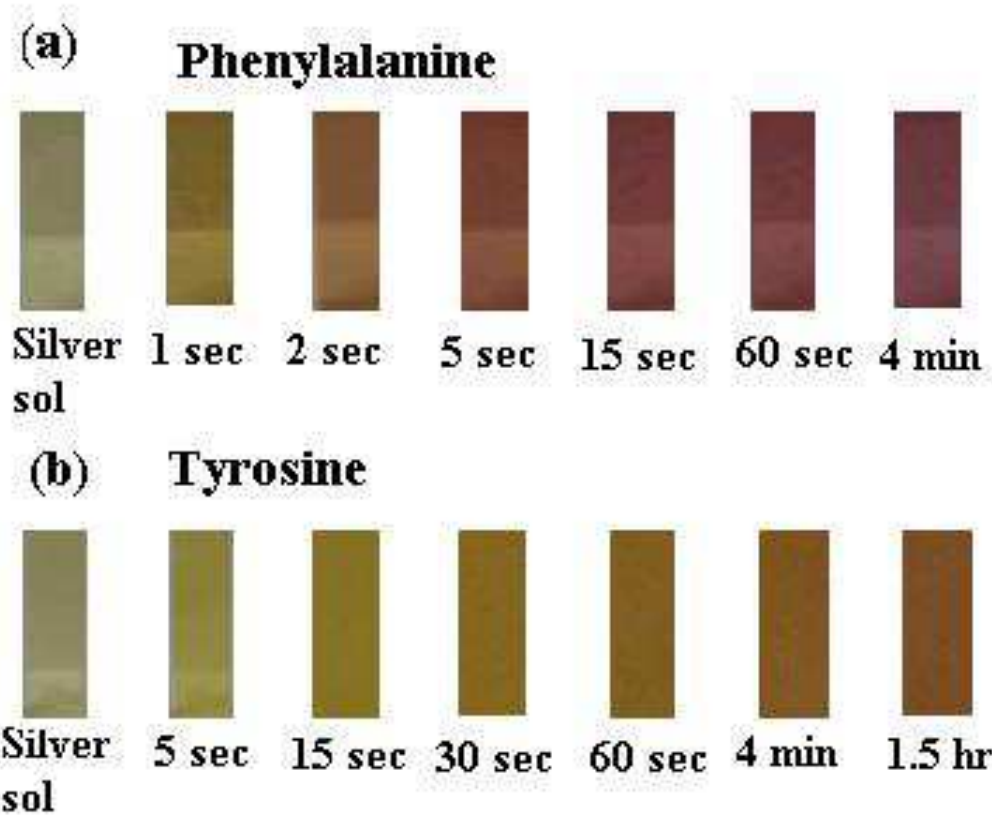


Figure 18. Singha et al